Hindawi
Geofluids
Volume 2018, Article ID 4034296, 14 pages
https://doi.org/10.1155/2018/4034296

Research Article

The Migration of Coalbed Methane under Mining Pressure and Air Injection: A Case Study in China

Liqiang Zhang,[1] **Yu Wu**,[1,2] **Hai Pu**,[1,2] **Xiaoping He**,[1] **and Pan Li**[1]

[1]*State Key Laboratory for Geomechanics and Deep Underground Engineering, China University of Mining & Technology, Xuzhou, Jiangsu 221008, China*
[2]*School of Mechanics and Civil Engineering, China University of Mining & Technology, Xuzhou 221116, China*

Correspondence should be addressed to Yu Wu; wuyu@cumt.edu.cn

Received 7 April 2018; Accepted 5 July 2018; Published 5 August 2018

Academic Editor: Wen Wang

Gas outburst has always affected the safety of coal mining. To eliminate this risk by high-efficiency extraction of coalbed methane (CBM) in 4102 working face of number 3 coal seam in Hebi Number 3 coal mine, a model of CBM extraction in working face was established which was considering the mining impact of adjacent 4101 working face. In this model, the coupling relationships between stress, desorption, and migration of methane were analyzed. Moreover, we also studied the changes of methane pressure, plastic failure scope, and permeability of coal during the mining and then verified the results with the field data. And on this basis, a stimulation solution for methane extraction by injecting air into coal seam was presented, and the extraction effect was simulated. The simulation results show that the injection of air decreases the effective stress of coal which increases the permeability of coal and promotes the methane migration within the coal seam fractures. Besides, affected by the velocity of gas migration, the pressure drop between fractures and matrix will reduce with time while air injection can provide extra power for gas migration in fractures which causes the desorption and diffusion of methane in the matrix. So this stimulation solution can enhance the efficiency of gas extraction of coal seam and prevent gas outburst of the working face.

1. Introduction

China has abundant coal resources and mainly depends on coal as energy [1]. Coalbed methane (CBM) is a companion gas of coal, and it is also a kind of low-carbon energy. According to the statistics of China Energy Bureau, the total geological reserves of CBM are about 10 billion m^3. In China, there are many problems on the extraction of CBM, such as slow methane pressure decreasing, rapid methane concentration reducing, and low permeability of coal seam. This makes it difficult to use the low concentration methane effectively which will be eventually discharged into the atmosphere. Efficient extraction of CBM and reduction of coal and gas outburst disasters have a profound impact on the simultaneous exploitation of coal and CBM [2].

Due to the advantages of easy construction, eliminating gas outburst risks, the technologies of drilling holes along and across coal seam are widely used in CBM extraction. Many studies indicate that methane migration is influenced by gas-solid coupling effect between mining pressure and gas pressure of coal seam [3]. The deformation of coal induced by mining pressure would change the pore volume of matrix, which leads to the change of coal seam permeability. To quantitatively analyze the influence of matrix shrinkage and expansion on coal permeability, Liu et al. [4] proposed a coupled model of permeability based on the gas adsorption/desorption experiments and then analyzed the effect of matrix shrinkage on permeability. Since then, many scholars have done different researches on the coal seam permeability model with gas-solid coupling. Gilman and Beckie

[5], Pillalamarry et al. [6], Chen [7], Sawyer et al. [8], and Seidle and Huitt [9] established relevant theoretical models of permeability based on different assumptions, respectively.

In the mining process, Huy et al. [10] considered that with the increase of effective stress, the fracture opening of coal seam decreases gradually and some microfractures were completely closed, which made the permeability decrease sharply. Liang [11] introduced the geological storage conditions of Huainan mining area and studied the related technology of CBM extraction and drainage boreholes. Shi et al. [12] studied the relationship between loading rate and borehole destruction and proposed that the layout of methane drainage boreholes should take into account the mining pressure. Yin et al. [13] studied the methane extraction process under the mining pressure of the adjacent working face. The results show that the gas flow rate gradually decreases with the increase of mining pressure. With the help of KSE gas concentration recorder and SF6 gas conveyor, Wang et al. [14] studied the gas-solid coupling phenomenon between mining pressure and gas migration. The results showed that the change of mining pressure is the key factor of permeability change in the coal seam. Based on the research background of Zhangji coal mine, Xue et al. [15] analyzed the influence of different mining methods on the permeability of coal seam. Wei et al. [16] also pointed out that the coal permeability showed a u-shaped curve change in the coal sample full stress-strain experiment.

In the previous studies, a series of theoretical models for methane extraction have been put forward on the safety of methane extraction. These models were applied to research the gas-solid coupling phenomenon in the process of methane extraction. However, most of the studies focused on the mechanism of gas migration and permeability change, and the influence of dynamic mining pressure change on the methane extraction in coal seam was seldom taken into account. In this study, we established a dual-porosity and dual-permeability methane drainage model with the periodic effect of mining pressure of the near working face to solve the specific problems in the methane drainage of 4102 working face in number 3 coal seam of Hebi Number 3 coal mine in China. The interaction relationship between gas and coal seam under the influence of mining was studied, and the methane concentration and flow rate were analyzed. On this basis, a solution to enhance the efficiency of methane extraction by injecting air was put forward. A simulation study was carried out to analyze the permeability change of coal seam and the gas migration rule after air injection.

2. Background of the Experimental Mine

2.1. Geological and Storage Conditions. Hebi Number 3 coal mine is located in Hebi City of Henan Province of China. Many coal and gas outburst accidents occurred since 1978. The geological conditions of number 3 coal seam are shown in Figure 1(a), 4101 working face is the first mining working face, and 4102 working face is prepared for eliminating the danger of gas outburst before mining. The burial depth of two working faces and the average thickness of number 3 coal seam are 784 m and 5.2 m, respectively. And the methane content of number 3 coal seam is about 10.92–8.96 m^3/t. The methane pressure measured in the field is between 1.58 and 2.36 MPa. Boreholes are drilled along the coal seam for methane extraction with a diameter of 94 mm, and negative extraction pressure is about 12–20 kPa.

2.2. Main Problems in Gas Extraction. In fact, in the related study of mining pressure and methane emission, it is considered that under the influence of abutment pressure, due to the effect of "relieving pressure and increasing permeability of coal" [17], it will accelerate the migration of gas in the fracture. Finally, the amount of methane emission will increase, which will help to eliminate the danger of gas outburst. In view of the actual methane extraction of the 4102 working face, especially affected by the mining activities of 4101 working face, the mining pressure value and position of the 4102 working face are constantly changed. At this point, it is necessary to further study the coupling effect between the coal permeability change, free gas migration, and adsorption deformation of 4102 working face.

As a gas outburst mine, Hebi Number 3 coal mine has taken a series of measures to eliminate coal and gas outburst, such as hydraulic fracturing and loose blasting of deep-hole explosives. At the same time, according to the regulations of coal mine safety, it is necessary to use the upward drilling of the roadway excavated in the floor of coal seam to extract methane technology [18]. But it is difficult to popularize because the effect of penetration and extraction cannot meet the requirement of mine safety production and the replacement of working face. Therefore, we have to take a more effective method to quickly reduce the methane pressure of coal seam.

3. Dual-Porosity Model for Methane Migration

3.1. Model Assumptions. The permeability of coal seam is the key influence factor for the methane extraction research. Compared with conventional natural gas reservoirs, the permeability of coal seam extracted by mines changes between 0.1 D and 0.001 mD ($1\,D = 10^{-12}\ m^2$) [19], which is completely different from the conventional natural gas extraction. In general, coal seam is a dual-porosity media containing matrix pores and fractures. Natural fractures of coal seam can be divided into horizontal bedding fracture and vertical cleat fracture. Methane is mainly stored in the pores by adsorbing on the micropore surface accounting for 70–95% [20, 21] of the total reserves. Free methane mainly migrates in coal seam fractures following the convection-diffusion equation. In the matrix system, there are many phenomena involved, but Fickian diffusion is the most dominant in the porous structure of the coal matrix [22, 23]. The main process of methane migration in the coal seam is shown in Figure 2.

In the following, a set of field equations for coal deformation, gas flow, and transport are defined. These field equations are coupled through new porosity and permeability

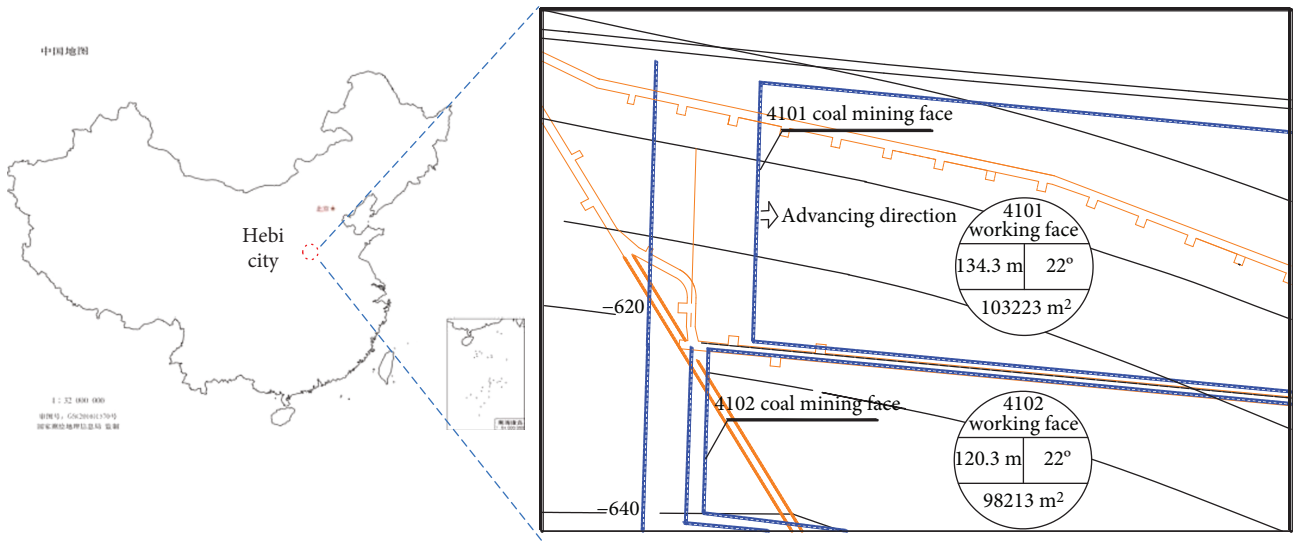

(a) Experimental coal mine location

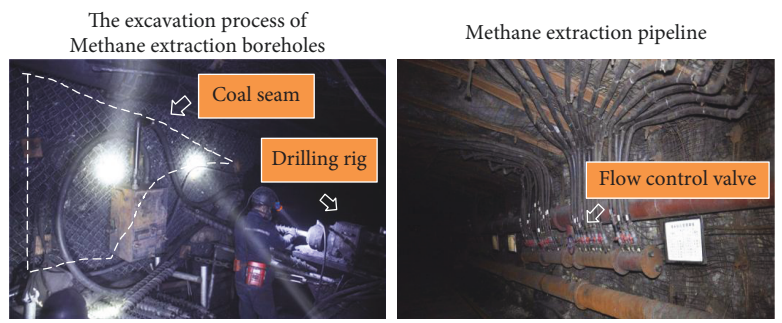

(b) Drilling and extraction pipeline of gas extraction in this coal seam

Figure 1: The location and extraction conditions of coal mining face.

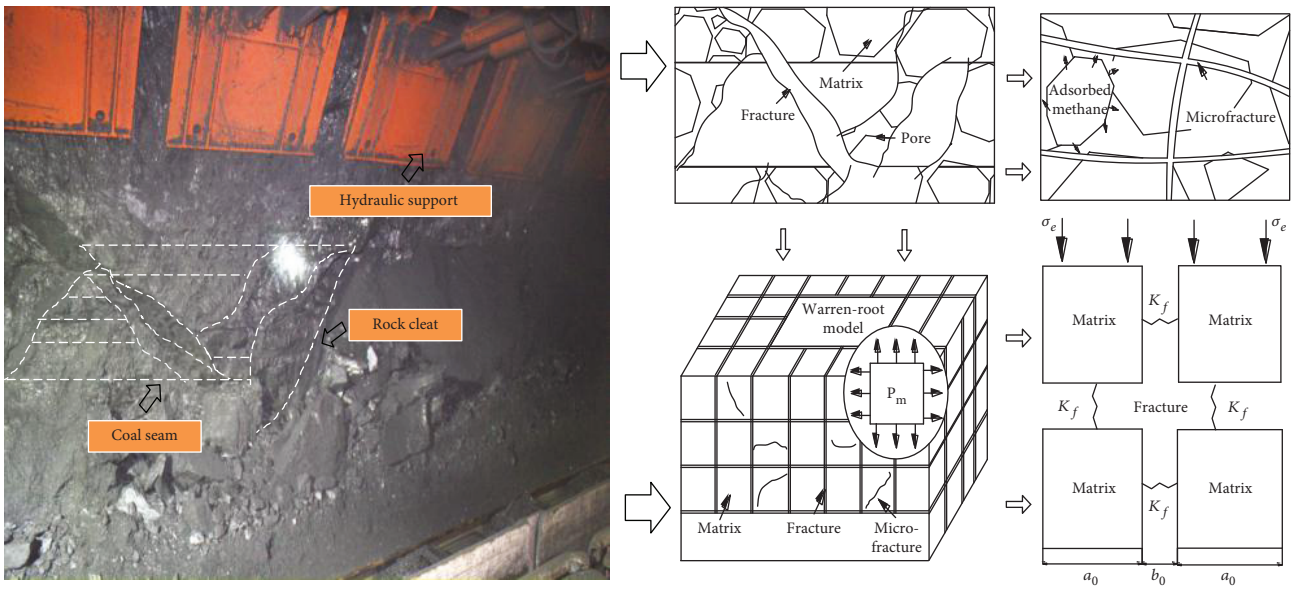

Figure 2: The process of methane migration in coal seam.

models for matrix and fractures. The derivations are based on the following assumptions:

(1) Coal is a dual-poroelastic continuum.

(2) The influence of coal seam moisture on gas migration is ignored.

(3) Methane contained in the pores is ideal gas, and its viscosity is constant under isothermal conditions.

(4) The air injected in coal seam is ideal saturated gas, and the adsorption effect of coal seam on air is ignored.

3.2. Coal Deformation Equation. As shown in Figure 1, the ideal simplified model of coal seam is composed by fractures and matrices. The matrices are composed by many primary pores. The deformation of this dual-porosity model can be represented by a Navier-type equation [24]:

$$Gu_i + \frac{G}{1-2\nu}u_k - \alpha p_{\text{mmix}} - \beta p_{\text{fmix}} - K\frac{\varepsilon_L P_L}{(P_L + P_{m1})^2} + F_i = 0, \tag{1}$$

where G, ν, and K are the shear modulus, Poisson's ratio, and bulk modulus of coal, respectively, α and β are the Biot coefficients of matrix and fracture, ε_s is gas sorption strain, and P_{mmix} and P_{fmix} are the pore pressure in fractures and matrix. The relationship of these parameters can be defined as follows:

$$\begin{aligned} G &= \frac{D}{2(1+\nu)}, \quad D = \left[\frac{1}{E} + \frac{1}{a_0 \cdot K_{\text{f}}}\right]^{-1}, \\ \alpha &= 1 - \frac{K}{K_{\text{s}}}, \\ \beta &= 1 - \frac{K}{a_0 \cdot K_{\text{f}}}, \\ \varepsilon_{\text{s}} &= \frac{\varepsilon_{\text{L}} p_{\text{m1}}}{p_{\text{m1}} + P_{\text{L}}}, \end{aligned} \tag{2}$$

where E is the elastic modulus of coal, K_{f} is the bulk modulus of fracture, K_{s} is the bulk modulus of matrix, K_{f} is the normal stiffness of fracture, F_i is the body force of element, usually is gravity, and ε_{L} and P_{L} are the Langmuir adsorption strain and pressure constants.

In (1), the first two terms represent the deformation of representative element volume (REV) under the influence of gas mixture pressure change and adsorption. The third and fourth terms represent the deformation of methane pressure in the matrix and fracture system, respectively. The fifth term represents the volume deformation due to the adsorption effect of matrix on gas.

3.3. Methane Migration Equation. According to Masoudian et al. [25], there are two types of coalbed methane reservoir models that may be used for methane flow in coal. The most primitive type is the diffusion which is assumed to be instantaneous, but this cannot fully describe the methane flow processes in coal seams. The second type, which is the most widely used for coalbed methane simulations, assumes coal is modeled with a dual-porosity system comprised of fractures and is microporous. Based on the methane migration speed, the model includes the Darcy convection equation for gas transfer in the fracture and Fick equation for gas diffusion in the matrix. The equation of gas mass transfers between them can be expressed as follows [26]:

$$\frac{\partial M_n}{\partial t} + \nabla(v_n \cdot \rho_n) - \nabla(D_n \cdot \nabla M_n) = Q_{\text{s}}, \tag{3}$$

where M is the mass of gas in coal seam; the subscript "n" ($n = 1, 2$) represents methane and air; v_n is the transfer velocity of gas in fracture; D_n is the diffusion coefficient of component gases; ρ_n is the gas density; t is the time; and Q_{s} is the term of gas source, usually regarded as the gas initial pressure.

Methane is mainly stored in matrix pores in adsorbed and free states. By ignoring the influence of matrix on the air, the mass of methane and air in matrix can be expressed as follows at any time [27]:

$$\begin{aligned} M_{\text{m1}} &= \rho_{\text{m1}}\phi_{\text{m}} + \rho_{\text{ga}}\rho_c\frac{V_{\text{L}} p_{\text{m1}}}{p_{\text{m1}} + P_{\text{L}}}, \\ M_{\text{m2}} &= \rho_{\text{m2}}\phi_{\text{m}}. \end{aligned} \tag{4}$$

Methane and air are mainly transferred in the fractures of coal, and the mass of mixed gas in the fractures can be expressed as follows at any time:

$$M_{\text{f}n} = \rho_{\text{g}n}\phi_f, \tag{5}$$

where M_{m1} is the mass (kg/m^3) of gas. The subscripts of "m" and "f" indicate the matrix and fracture, respectively; ρ_{ga} is the gas density at standard atmospheric pressure (kg/m^3); ρ_{c} is the density of coal (kg/m^3); P_{L} is the Langmuir adsorption pressure constant (MPa); V_{L} is the Langmuir adsorption volume constant (m^3/t); ϕ_{m} is the matrix porosity (%); $\rho_{\text{m}n}$ is the density of gas in the matrix, $\rho_{\text{m}n} = m_n P_{\text{m}n}/RT$; $\rho_{\text{f}n}$ is the density of gas in the fracture, $\rho_{\text{f}n} = m_n P_{\text{f}n}/RT$.

In regard to the term of gas migration in (4), the convection velocity of any gas can be expressed as follows (ignoring the effect of gravity):

$$\begin{aligned} v_{\text{f}n} &= \frac{k_{\text{f}}}{u}\nabla p_{\text{fmix}}, \\ v_{\text{m}n} &= \frac{k_{\text{m}}}{u}\nabla p_{\text{mmix}}, \end{aligned} \tag{6}$$

where k_{f} and k_{m} are the fracture permeability and matrix permeability, respectively; u is the dynamic viscosity of gas mixture; and ∇p_{f} and ∇p_{m} are the pressure difference of gas flow in the fracture and matrix. Substituting (4), (5), and (6) into (3), the gas mixture flow control equation can be obtained.

$$\left[\phi_m + \rho_c p_{ga}\frac{V_L P_L}{(p_{m1}+P_L)^2}\right]\frac{\partial p_{m1}}{\partial t} + p_{m1}\frac{\partial \phi_m}{\partial t} = \nabla\left(p_{mmix}\frac{k_m}{u}\nabla p_{mmix}\right) + \nabla(D_1\phi_m\nabla m_1) - \omega(p_{mmix}-p_{fmix}), \tag{7}$$

$$\phi_f\frac{\partial p_{f1}}{\partial t} + p_{f1}\frac{\partial \phi_f}{\partial t} - \nabla\left(p_{fmix}\frac{k_f}{u}\nabla p_{fmix}\right) - \nabla(D_1\phi_f\nabla m_1) = \omega(p_{mmix}-p_{fmix}), \tag{8}$$

$$\phi_m\frac{\partial p_{m2}}{\partial t} + p_{m2}\frac{\partial \phi_m}{\partial t} - \nabla\left(p_{mmix}\frac{k_m}{u}\nabla p_{mmix}\right) - \nabla(D_2\phi_m\nabla m_2) = -\omega(p_{mmix}-p_{fmix}), \tag{9}$$

$$\phi_f\frac{\partial p_{f2}}{\partial t} + p_{f2}\frac{\partial \phi_f}{\partial t} - \nabla\left(p_{fmix}\frac{k_f}{u}\nabla p_{fmix}\right) - \nabla(D_2\phi_f\nabla m_2) = \omega(p_{mmix}-p_{fmix}), \tag{10}$$

where $\omega = 8[1+(2/a_0{}^2)]k_m/\mu$ is the exchange coefficient between matrix and fracture [28] and a_0 is the initial fracture width.

3.4. Dynamic Permeability Model of Coal Seam. For CBM extraction, the effective stress change and methane desorption cause deformation of the coal; Palmer and Mansoori, Shi and Durucan [29], and Cui and Bustin [30] had proposed a dynamic variation model of permeability based on different assumptions. On the basis of summarizing the development and application of coalbed methane, Pan and Connell [31] analyzed the existing reservoir permeability model and analyzed that the change of permeability is an important physical parameter for evaluating the extraction of coalbed methane. Mohsen et al. [32] also pointed out that the permeability model under vertical stress change should be considered and needs to find a balance between the complexity of the permeability model and the accuracy of the field permeability data. In this study, we use the dynamic permeability variation model proposed by Wu et al. [33] to study the CBM extraction under the mining pressure. However, unlike Wu's model, the coupling effect of gas mixture pressure and different cycle mining pressures on gas migration was studied in this paper. The equation of coal seam matrix permeability can be expressed as

$$\phi_m = \alpha + (\phi_{m0}-\alpha)\exp\left[\frac{1}{K}\left(\frac{1}{K}+\frac{b_0}{a_0K_f}\right)^{-1}(\varepsilon_V-\varepsilon_{V0}-\varepsilon_S+\varepsilon_{S0})\right], \tag{11}$$

where ϕ_m is the real-time porosity of the matrix and the subscript "0" indicates the initial state; $\varepsilon_V = \varepsilon_{11}+\varepsilon_{22}+\varepsilon_{33}$ indicates the deformation of the representative element volume; and $\varepsilon_S = \varepsilon_L p_{m1}/(p_{m1}+P_L)$ is the gas adsorption strain in pores.

In the same way as above, the porosity of coal seam fracture system can be expressed as

$$\frac{\phi_f}{\phi_{f0}} = 1 + \frac{1}{K_f}\left(\frac{1}{K}+\frac{b_0}{a_0K_f}\right)^{-1}(\varepsilon_V-\varepsilon_{V0}-\varepsilon_S+\varepsilon_{S0}). \tag{12}$$

During the methane extraction, with the continuous decrease of gas pressure, the pore volume of matrix changes continuously with time. The equation for porosity change within the matrix over time can be written as

$$\frac{\partial \phi_m}{\partial t} = (\phi_m-\alpha)\exp\left[\frac{1}{K}\left(\frac{1}{K}+\frac{b_0}{a_0K_f}\right)^{-1}\left(\frac{\partial \varepsilon_V}{\partial t}-\frac{\partial \varepsilon_S}{\partial t}\right)\right], \tag{13}$$

$$\frac{\partial \phi_f}{\partial t} = \frac{\phi_{f0}}{K_f}\left(\frac{1}{K}+\frac{b_0}{a_0K_f}\right)^{-1}\left(\frac{\partial \varepsilon_V}{\partial t}-\frac{\partial \varepsilon_S}{\partial t}\right). \tag{14}$$

The permeability and porosity of coal seam matrix and fracture can be expressed in the cubic formula:

$$\frac{k_f}{k_{f0}} = \left(\frac{\phi_f}{\phi_{f0}}\right)^3 = \left[1+\frac{1}{K_f}\left(\frac{1}{K}+\frac{b_0}{a_0K_f}\right)^{-1}(\varepsilon_V-\varepsilon_{V0}-\varepsilon_S+\varepsilon_{S0})\right]^3,$$
$$\frac{k_m}{k_{m0}} = \left(\frac{\phi_m}{\phi_{m0}}\right)^3 = \left[1-\frac{\alpha}{K\phi_{m0}}\left(\frac{1}{K}+\frac{b_0}{a_0K_f}\right)^{-1}(\varepsilon_V-\varepsilon_{V0}-\varepsilon_S+\varepsilon_{S0})\right]^3, \tag{15}$$

where k_{f0} and k_{m0} are the initial permeability of the fracture and matrix (in m^2).

3.5. Coupled Field Equations. By substituting (13) and (14) into (7), (8), (9), and (10) of gas flow, respectively, the final equation of gas flow control equations can be expressed as

$$\left[\phi_m + (1-\phi_{m0})\frac{\rho_c p_{ga}P_L V_L}{(p_{m1}+P_L)^2} - \left(\frac{\alpha K_f}{(b_0/a_0)K+K_f}\right)\left(\frac{P_L\varepsilon_L p_{m1}}{(p_{m1}+P_L)^2}\right)\right]\frac{\partial p_m}{\partial t} = \nabla\left(\frac{k_m}{u}p_{mmix}\nabla p_{mmix}\right) + \nabla(\phi_m D_1\nabla p_{mmix}) + 8\left(1+\frac{2}{a_0{}^2}\right)\frac{k_m}{\mu}(p_{f1}-p_{m1}) - \left(\frac{\alpha K_f}{(b_0/a_0)K+K_f}\right)\left(p_{m1}\frac{\partial \varepsilon_v}{\partial t}\right), \tag{16}$$

$$\begin{aligned}\phi_f \frac{\partial p_{f1}}{\partial t} &- \nabla\left(\frac{k_f}{u} p_{fmix} \nabla p_f\right) - \nabla(\phi_f D_1 \nabla p_{fmix}) \\ &= -8\left(1 + \frac{2}{{a_0}^2}\right)\frac{k_m}{\mu}(p_{f1} - p_{m1}) \\ &\cdot - \frac{3\phi_{f0} p_{f1}}{\phi_{f0} + (3K_f/K)} \\ &\cdot \left[\frac{\partial \varepsilon_v}{\partial t} - \frac{\varepsilon_L P_L}{(p_{m1} + P_L)^2}\left(\frac{\partial p_{m1}}{\partial t}\right)\right],\end{aligned} \tag{17}$$

$$\begin{aligned}\phi_m \frac{\partial p_{m2}}{\partial t} &- \nabla\left(\frac{k_m}{u} p_{mmix} \nabla p_{mmix}\right) - \nabla(\phi_m D_2 \nabla p_{mmix}) \\ &= 8\left(1 + \frac{2}{{a_0}^2}\right)\frac{k_m}{\mu}(p_{f2} - p_{m2}) + p_{m2} \\ &\cdot \left(\left(\frac{\alpha}{K}\right)\left(\frac{1}{(1/K_f) + (b_0/a_0 K)}\right)\right) \\ &\cdot \left[\left(\frac{P_L \varepsilon_L}{(p_{m1} + P_L)^2}\right)\frac{\partial p_{m1}}{\partial t} - \frac{\partial \varepsilon_V}{\partial t}\right],\end{aligned} \tag{18}$$

$$\begin{aligned}\phi_f \frac{\partial p_{f2}}{\partial t} &- \nabla\left(\frac{k_f}{u} p_{fmix} \nabla p_{fmix}\right) - \nabla(\phi_f D_2 \nabla p_{fmix}) \\ &= -8\left(1 + \frac{2}{{a_0}^2}\right)\frac{k_m}{\mu}(p_{f2} - p_{m2}) - \frac{p_{f2}\phi_{f0}}{K_f} \\ &\cdot \left(\frac{1}{K} + \frac{b_0}{a_0 K_f}\right)^{-1}\left[\frac{\partial \varepsilon_V}{\partial t} - \left(\frac{P_L \varepsilon_L}{(p_{m1} + P_L)^2}\right)\left(\frac{\partial p_{m1}}{\partial t}\right)\right].\end{aligned} \tag{19}$$

Equations (16), (17), (18), and (19) describe the flow of mixed gas within fracture of coal seam under mining pressure. In (16), the first term $\partial p_m/\partial t$ at the left is composed of three subterms sequentially including (I) pressure variation of free gas in matrix pores; (II) deformation of the matrix caused by gas desorption; and (III) deformation of fracture volume. The third and fourth terms on the right of the equation indicate the exchange of free gas between the fracture and matrix, methane released by the deformation of coal. The first term on the left of (17) represents the pressure variation of methane in the fracture. The second term on the right of the equation contains two subterms, that is, the effect of coal seam volume deformation on gas and the effect of methane desorption strain. The physical meanings of (18) and (19) are the same as those of (16) and (17). The above coupling control equations contain the terms of time and space derivation, which need to be solved by Comsol Multiphysics. The interaction between the physical fields is shown in Figure 3.

4. Gas Migration Characteristics under the Mining Pressure

4.1. Numerical Model and Input Parameters. The model is established based on a section of 4102 working face of number 3 coal seam with dimensions of 40 m (length) × 5 m (height). Negative-pressure drainage boreholes were drilled in advance and arranged in the horizontal center of number 3 coal seam. The diameter of boreholes is 100 mm, and the horizontal spacing is 3 m. The numerical model of the 4102 working face is shown in Figure 4 and the input parameters in Tables 1 and 2 as required. In this part, we only simulated the methane extraction under mining pressure.

As the advancing of 4101 working face, the mining pressure applied in 4102 working face would change as shown in Figure 5. In order to present the mining pressure, the pressure applied on the top of model can be divided into three iteration cycles. When the 4101 working face advanced by 10 meters totally, the mining pressure boundary was set again and the advance repeated in sequence until the end of the methane extraction. The initial pressure of methane in the coal (fracture and matrix) was set to 2 MPa, and the air pressure was set to 0 MPa. The migration of methane into the boreholes was only considered. Three points of A, B, and C of the model were selected as the data source for postprocessing with coordinates of (0.2, 2.5), (22.5, 2.5), and (39.8, 2.5).

4.2. Simulation Results. Under the influence of the mining in the 4101 working face, the initial stress equilibrium state of the coal seam is broken, and the different stress distribution regions are formed along the direction of the coal seam, which further affected the permeability of the coal seam. In the vicinity of gas drainage holes, there were three zones, that is, plastic failure zone, stress concentration zone, and original rock stress zone [34]. The permeability variations at the plastic failure zone and data points around the boreholes on both sides of the model are shown in Figure 6.

As shown in Figure 6(a), the permeability in the abutment pressure zone (right side of the model) was significantly lower than that in the original rock stress zone. During the whole extraction time, the variation of permeability was affected by the effective stress ($F_y - P_{fmix}$) and the strain of methane desorption. The permeability of coal seam (K_f) depends on the competition between them. In the early stage of extraction, the effective stress near the abutment pressure zone was obviously higher than the original rock stress zone, so the permeability was lower than that of other zones inhibiting the gas migration. With the increase in extraction time, the gas in adsorbed state was desorbed gradually, resulting in matrix shrinkage and gradual increase in the permeability. At the end of extraction, the permeability of coal seam in the original rock stress zone changed by about 5% (0.8–1.2). In the vicinity of the drainage boreholes, the drilling and excavation improved the expansion and extension of the original fractures leading to a sharp increase in the gas permeability of the coal seam. The permeability of the coal seam was significantly higher than the external permeability, and the fracture permeability increased by 5 times (0.8–4). The fractures in plastic failure zone became the dominant factor of permeability.

Figure 7 shows the methane pressure distribution at different extraction times. The gas migration during the extraction represented a typical gas-solid coupling. In the effect of extraction negative pressure, the gas pressure showed an exponentially decreasing trend. The trend line of methane pressure at point C went down significantly faster than that in the matrix. The decrease rate of gas pressure at point C

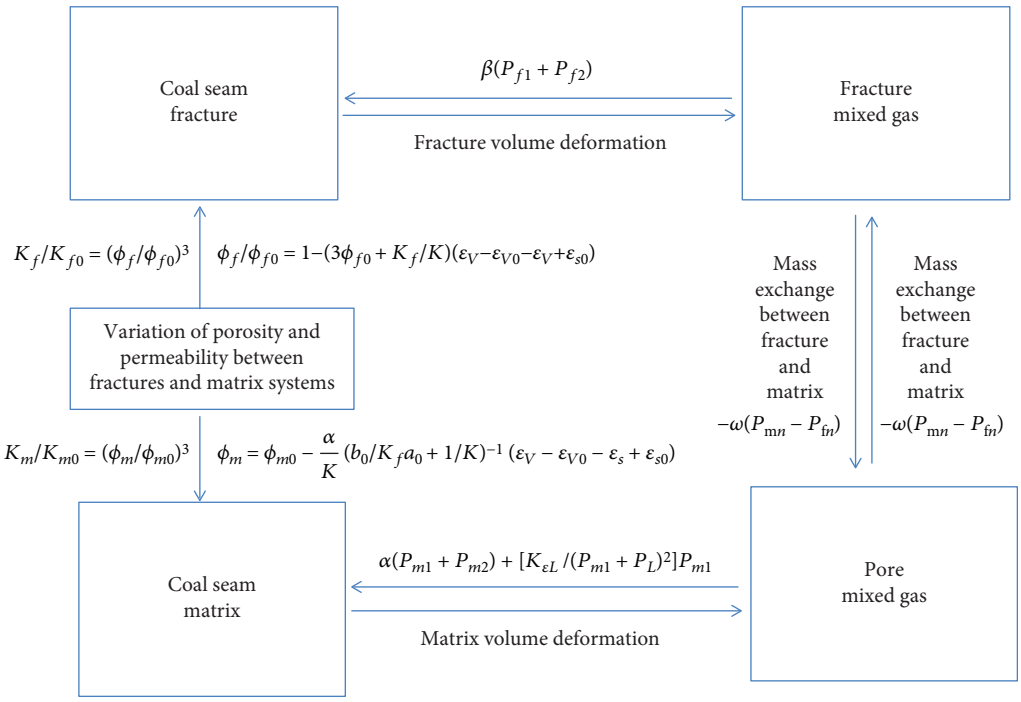

Figure 3: Coupling relationship between coal deformation and methane migration.

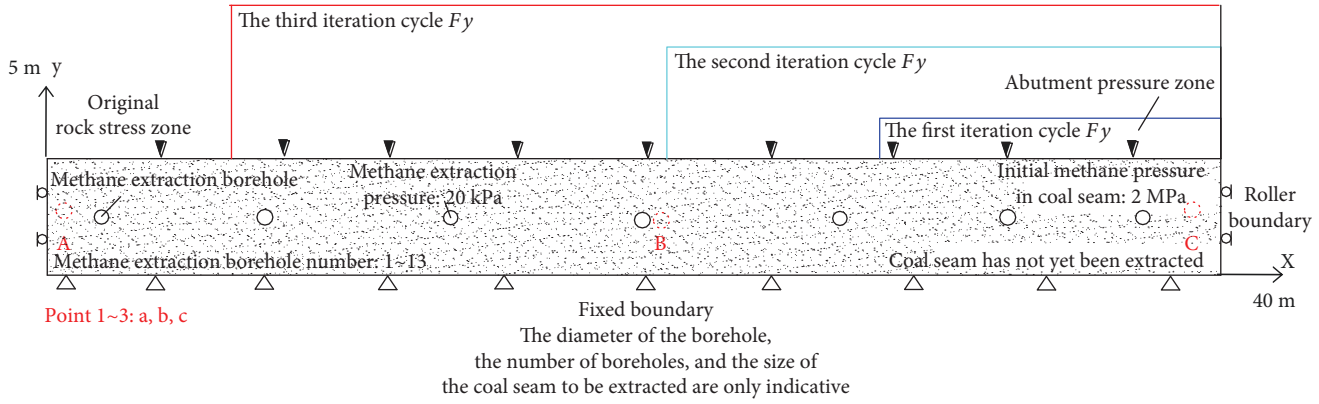

Figure 4: Numerical model of methane extraction in 4102 working face.

Table 1: Numerical model physical parameters.

Parameter	Value	Parameter	Value
Coal elastic modulus E (MPa)	2813	Adsorption pressure constant P_L (MPa)	2.07
Matrix elastic modulus E_s (MPa)	8439	Adsorption volume constant V_L (m^3/kg)	0.0256
Poisson's ratio ν	0.34	Adsorption pressure strain ε_L	0.015
Coal density ρ_c (kg/m^3)	1250	Initial matrix porosity. φ_{m0}	0.05
Air density (kg/m^3)	0.717	Initial matrix permeability k_{m0}	$2.8{\cdot}10^{-18}$
Facture stiffness K_f (MPa)	4800	Methane diffusion rate D_n (m^2)	$3.6{\cdot}10^{-12}$
Dynamic viscosity u (Pa·s)	$1.84{\cdot}10^{-5}$	Initial fracture porosity φ_{f0}	0.002
Bulk modulus K (MPa)	5400	Initial fracture permeability k_{f0}	$2.08{\cdot}10^{-17}$
Matrix width a_0 (m)	$5{\cdot}10^{-6}$	Initial temperature T (K)	300
Frack width b_0 (m)	0.005	Air diffusion rate D_n (m^2)	$5.8{\cdot}10^{-12}$

Table 2: Numerical model boundary conditions.

Coal seam deformation	Value	Methane migration	Value
Upper boundary (MPa)	14 transition to 21		
Lower boundary	Fixed boundary	Pressure of methane extraction borehole (kPa)	20
Left boundary	Roller support		
Right boundary		Methane pressure (MPa)	2
Borehole boundary	Free deformation		
Initial displacement	0	Others (MPa)	0

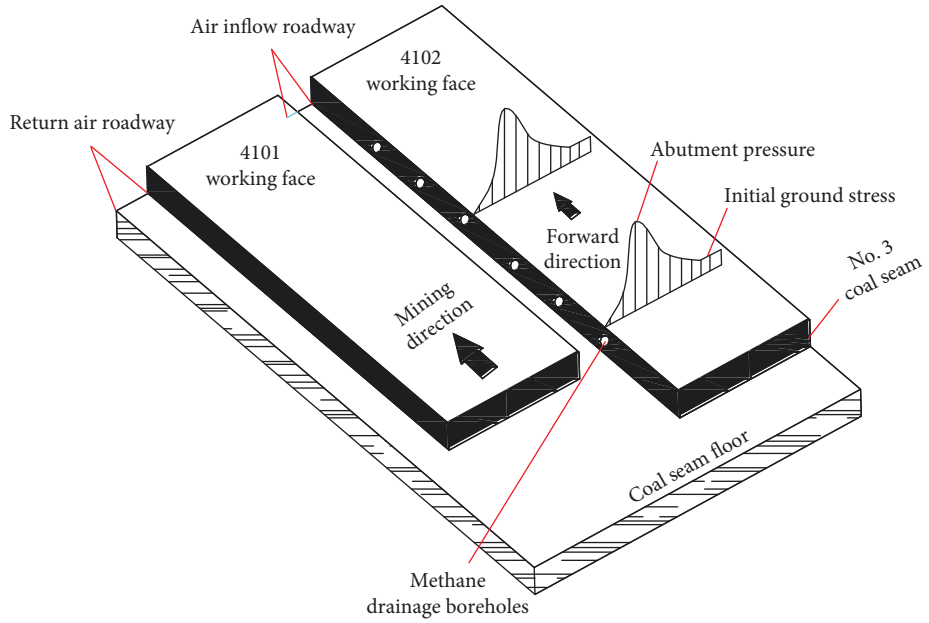

Figure 5: 4102 preparation work face.

was significantly slower than that at point B as the effective pressure of the coal seam was higher and the opening of the original fractures was smaller in the abutment pressure zone. The methane pressure difference ($P_m - P_f$) significantly increased at the early stage of the extraction (10 days ago) as there was pressure difference of gas transferred between the matrix and fracture. At the late stage of the extraction, the gas pressure difference gradually decreased until it was zero.

4.3. Comparisons with Field Data. The field data of methane pressure at number 1 and number 3 drainage boreholes were collected as shown in Figure 1. The methane pressure data obtained from the model were compared with the field data as shown in Figure 8. In the figure, although the methane pressure showed an overall decreasing trend, its downward trend was affected by the geological and storage conditions of the coal seam and the negative pressure of the drainage drilled holes resulting in fluctuations in pressure. The methane extraction numerical model was established with ideal conditions, ignoring the ash content and moisture in coal seam or other geological factors. Although their data were different, their curves showed the same change trend. This model can be used to predict and evaluate the long-term effect of borehole gas extraction.

5. Enhanced Gas Extraction Test by Injection Air

5.1. Air Injection Parameters. To eliminate gas outburst risks and reduce methane pressure as soon as possible, by injecting air into the existing boreholes of the 4102 working face, the gas migration was improved in the coal seam to increase the methane extraction effect. Figure 9 shows the injection boundary conditions and drilled boreholes in the model. The deformation field of the coal seam was established with the same settings as that of Section 4.1. The calculation parameters required by the model were the same as those in Table 1, and the air transport equation is shown in Table 3.

5.2. Gas Pressure Distribution. Figure 10 shows the effect of injection air pressure on methane pressure drop. The dotted line in the figure shows the change of methane pressure without air injection, and the solid line shows the change

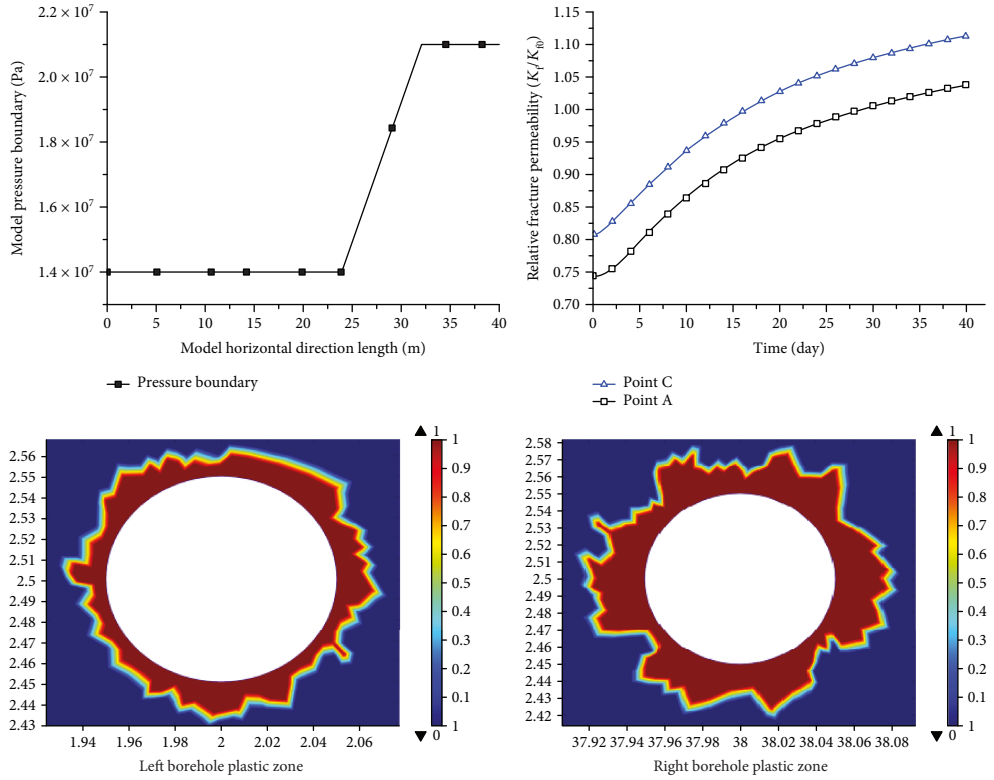

(a) The first calculation step, permeability, and plastic zone change

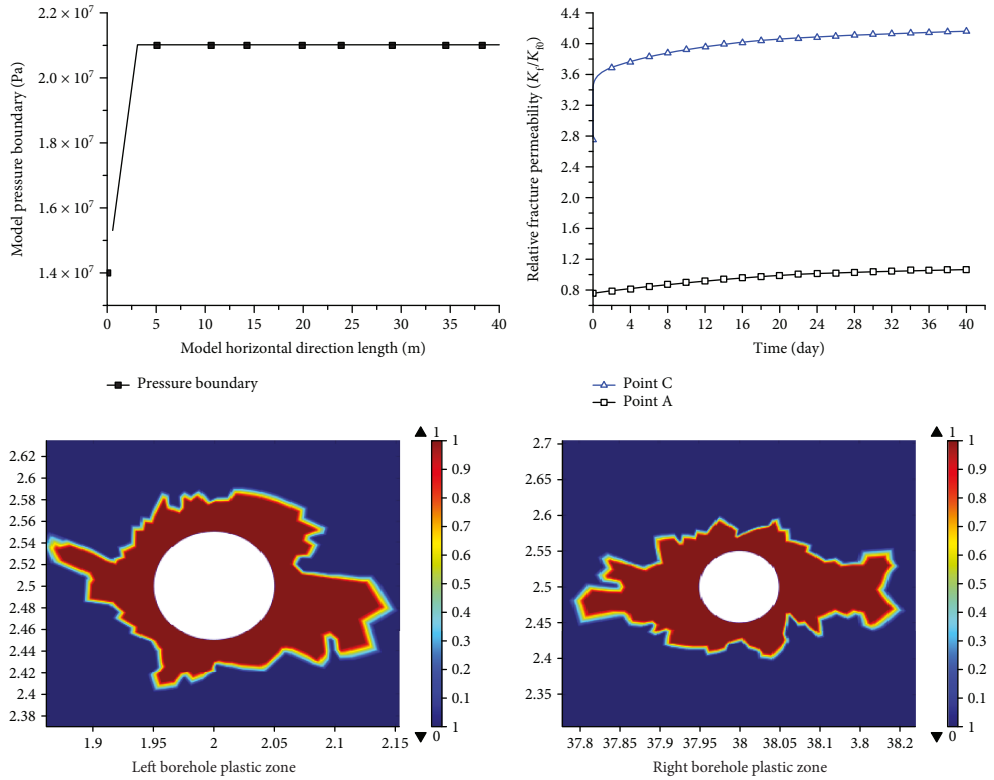

(b) The last calculation step, permeability, and plastic zone change

Figure 6: Different calculation steps, permeability, and plastic zone distribution.

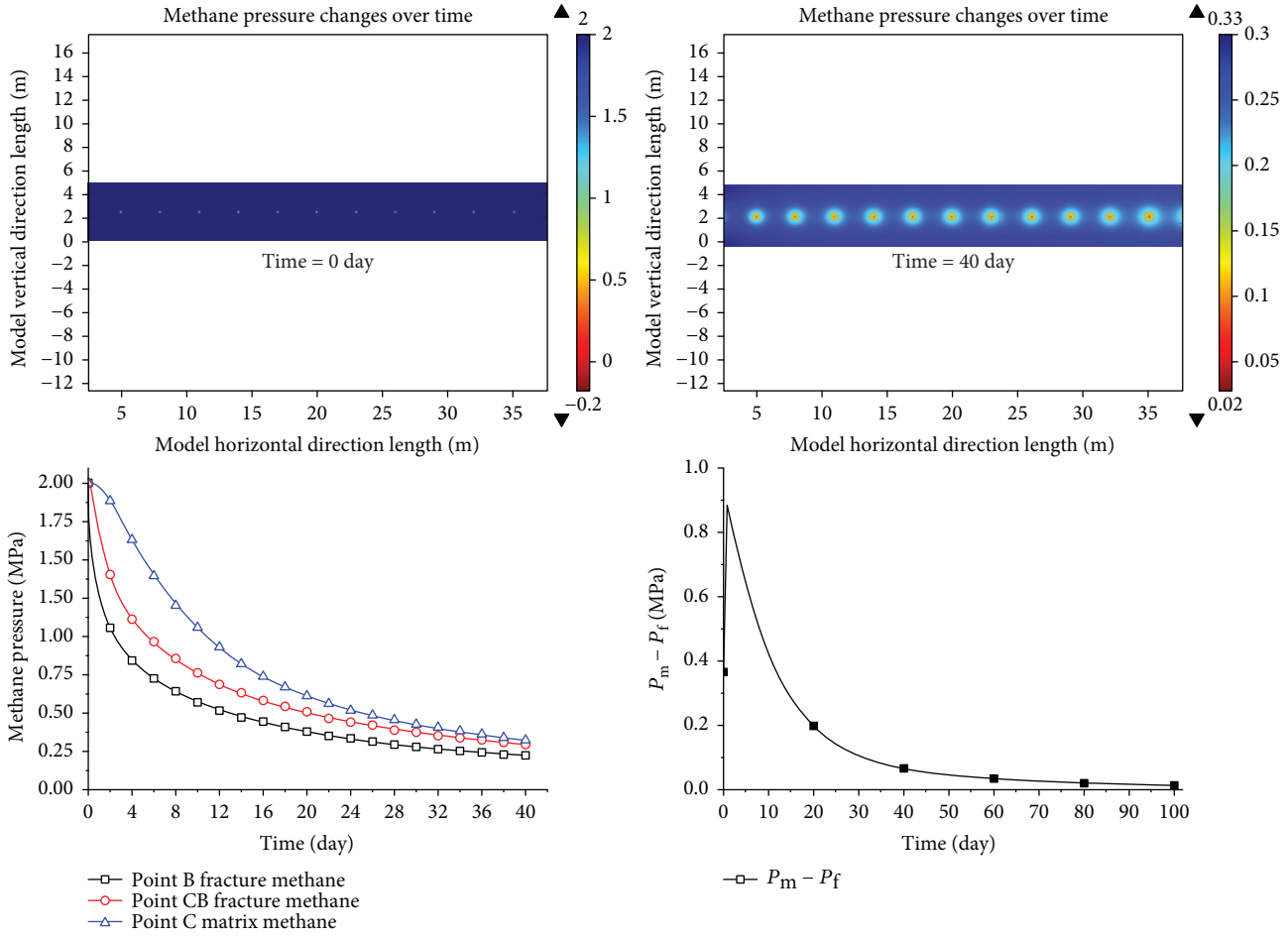

Figure 7: Coal seam methane pressure changes with time.

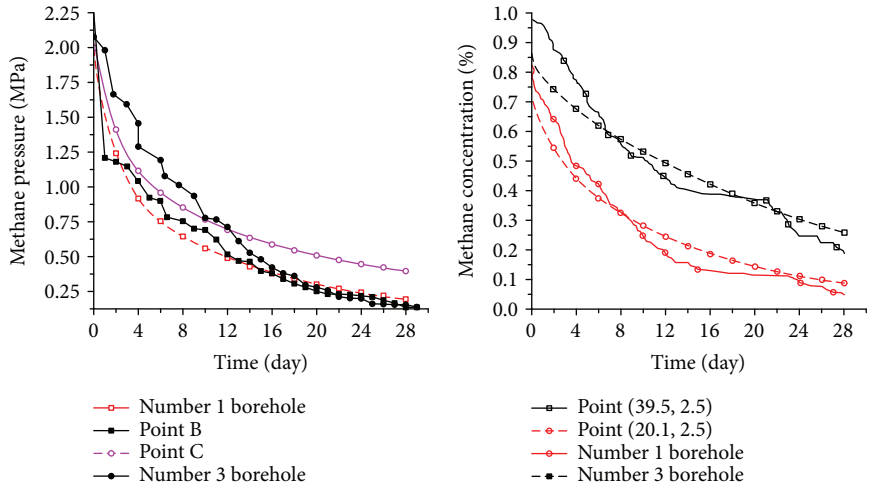

(a) Methane pressure varies with extraction time (b) Methane concentration changes with the time

Figure 8: Comparison of field methane pressure and numerical model results.

of methane pressure under different injected air pressures. When there was no air injected into the coal seam, the methane pressure at point C decreased to the safety pressure of 0.75 MPa, which took about 12 days. When the air pressure was increased to 1 MPa, the methane pressure decreased to 0.75 MPa, which only took about 8 days. The injection of air could significantly reduce the methane pressure.

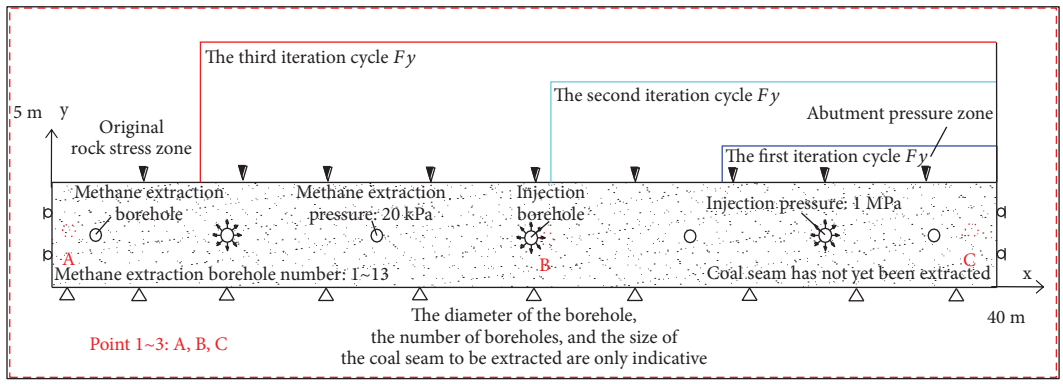

Figure 9: Setting of numerical model for methane extraction under air injection.

Table 3: Air migration equation setting.

Air migration	Value	Injection borehole position	Value
Initial pressure (MPa)	0	Extraction borehole number	1, 3, 5, 7, 9, 11
Injection pressure (MPa)	0.3, 0.6, 1		
Borehole boundary	Free deformation	Air injection borehole number	2, 4, 6, 8, 10
Initial displacement	0		

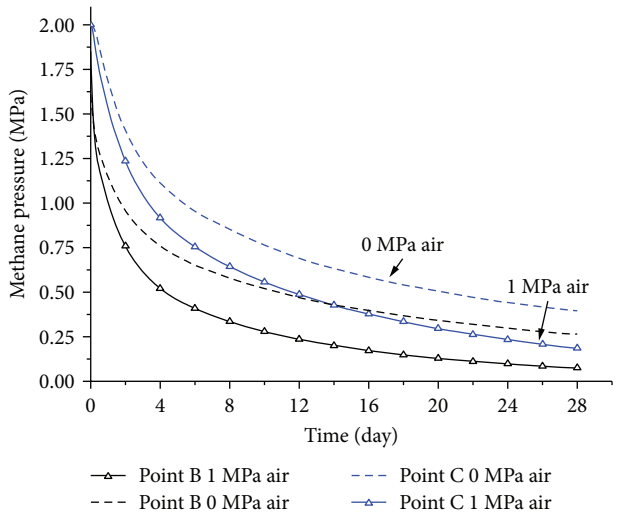

Figure 10: Methane pressure changes with time during air injection.

5.3. Evaluation of Coal Seam Permeability. Figure 11 shows the change trend of fracture permeability of coal seam at points B and C. During the whole extraction period, the permeability at the two points showed an increasing trend. When the air pressure in the fracture continued to increase, the effective stress of the coal seam continuously decreased, so the permeability at point B in the initial stage of injection was significantly higher than that at point C without injection. After 30 days of air injection, the air pressure in the model reached an equilibrium; the coal seam permeability at points B and C increased by 10% and 8%, respectively, compared to that in the initial stage of the extraction.

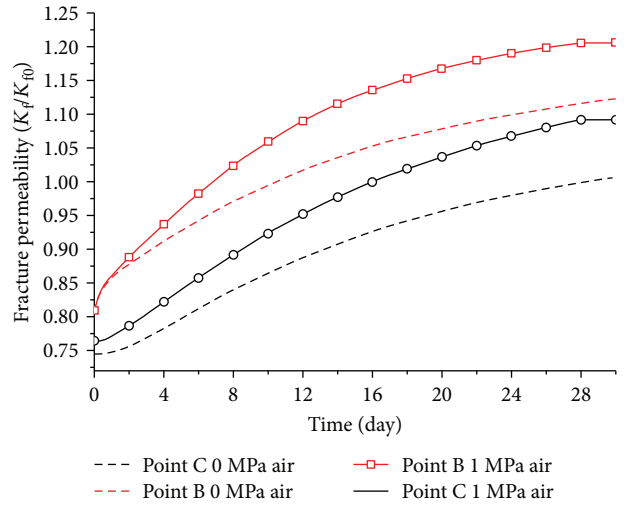

Figure 11: Coal seam permeability change under air injection.

5.4. Gas Flow Characters in Fracture. Figure 12 shows the variation of methane concentration. In the figure, the solid black line represents the methane concentration which decreased slowly when there was no air injection and showed an approximately linear decreasing trend in the extraction. After 15 days of extraction, the concentration only decreased by about 23%. The methane concentration decreased by 50% and 80%, respectively, compared with that under the air injection pressure of 0.6 MPa and 1 MPa in the condition that the extraction time was the same. By comparing the drop curve of methane pressure at point B in Figure 10, the methane pressure decreased to less than half of the initial value.

Figure 13 shows the variation of air concentration at point B and the change curves of methane flow rate under different air pressures. Figure 13(b) shows that the methane flow rate was significantly affected by the air pressure, that is, the higher the air pressure, the faster the methane flow rate at point B decreased. This was because the increasing of air pressure provided an additional power for methane to migrate in the fracture. Meanwhile, the fracture permeability was affected by the deformation of adsorbed methane desorption and the volume deformation of the coal. The desorption of methane caused continuous shrinkage of matrix eventually

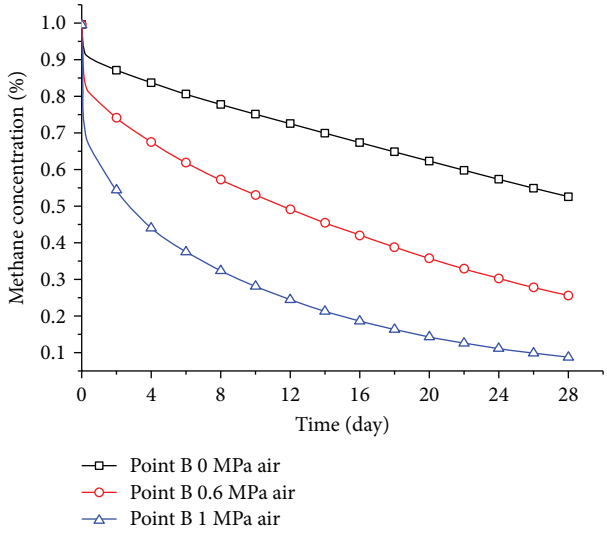

Figure 12: Methane concentration varies with time.

improving the permeability by 10% (Figure 11). The additional air pressure and permeability improvement accelerated the flow of methane in the fracture.

6. Conclusions

To study the impact of mining pressure on the methane extraction in coal, a dual-porosity and dual-permeability model was established with gas seepage, effective stress, and adsorption deformation. The gas-solid coupling between methane migration and borehole damage under the influence of abutment mining pressure was studied. On this basis, a stimulation treatment for methane extraction by injecting air was presented. Based on this study, the following conclusions can be obtained:

(1) When the boreholes are affected by the abutment mining pressure, the plastic failure zone around the boreholes increases the permeability of the coal and promotes the methane pressure drops rapidly, eliminating the danger of gas outbursts. On the contrary, radial extension along the boreholes, especially in the abutment pressure zone, with the increase of effective stress, not only the permeability decreases continuously but also limits the methane migration within the fracture. In the original rock stress zone, the change trend of coal permeability is between plastic failure zone and abutment pressure zone.

(2) The simulation results show that the methane in the fracture first flows into the drainage boreholes, then the methane in the matrix gradually diffuses. This is the reason why the methane pressure within coal is not on average always decreasing. Compared with the field data, the correctness of the methane drainage model under the abutment pressure near the working face was verified.

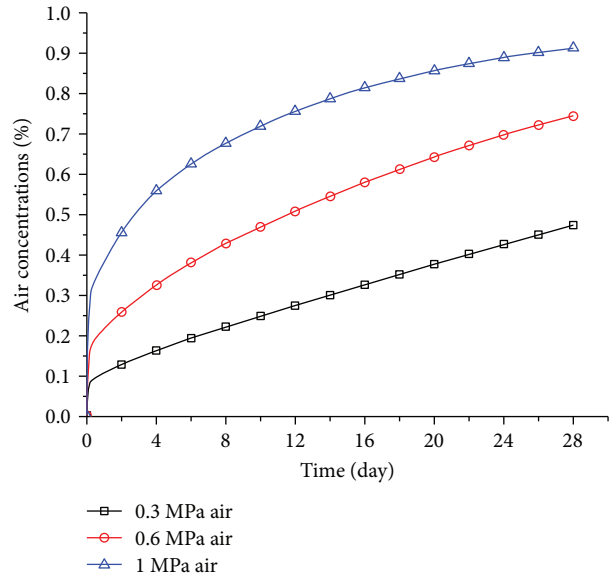

(a) Air concentration varies with time

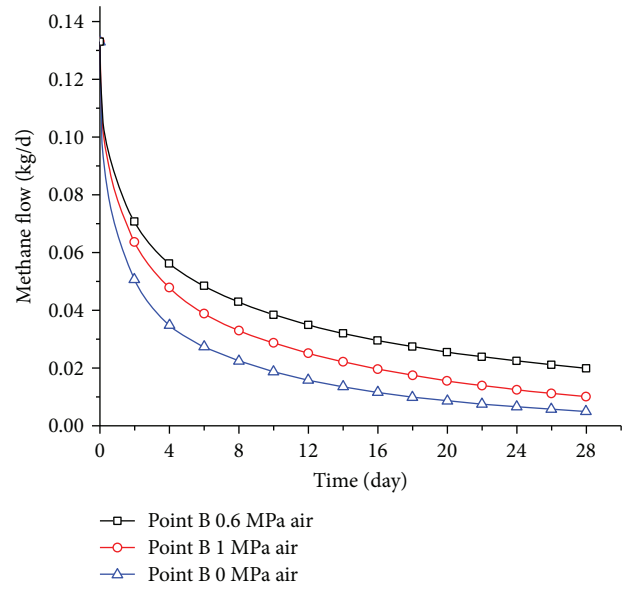

(b) Methane flow rate changes with the time

Figure 13: Methane flow rate changes with time.

(3) When air is injected into the coal, it first flows into the fractures and then reduces the effective stress of the coal, caused the fracture opening to increase continuously, and finally improves the permeability of coal. Extra air provides a new source of power for gas flow and promotes the flow of gas into the boreholes at the same time. This is the reason why the methane pressure within the fracture is always decreasing.

Data Availability

The data used to support the findings of this study are available from the corresponding author upon request.

Conflicts of Interest

The authors declare that they have no conflicts of interest.

Acknowledgments

This work was supported by the Fundamental Research Funds for the Central Universities (China University of Mining and Technology) with Grant 2015XKZD06 and National Natural Science Foundation of China with Grant 51674247. This work was also supported by the iCET (International Clean Energy Talent) Program from China Scholarship Council. These sources of support are gratefully acknowledged.

References

[1] J. Dong, Y. Cheng, K. Jin et al., "Effects of diffusion and suction negative pressure on coalbed methane extraction and a new measure to increase the methane utilization rate," *Fuel*, vol. 197, pp. 70–81, 2017.

[2] R. Pan, Y. Cheng, L. Yuan, M. Yu, and J. Dong, "Effect of bedding structural diversity of coal on permeability evolution and gas disasters control with coal mining," *Natural Hazards*, vol. 73, no. 2, pp. 531–546, 2014.

[3] J. Y. Jiang, Y. P. Cheng, L. Wang, W. Li, and L. Wang, "Petrographic and geochemical effects of sill intrusions on coal and their implications for gas outbursts in the Wolonghu Mine, Huaibei Coalfield, China," *International Journal of Coal Geology*, vol. 88, no. 1, pp. 55–66, 2011.

[4] H. H. Liu and J. Rutqvist, "A new coal-permeability model: internal swelling stress and fracture–matrix interaction," *Transport in Porous Media*, vol. 82, no. 1, pp. 157–171, 2010.

[5] A. Gilman and R. Beckie, "Flow of coal-bed methane to a gallery," *Transport in Porous Media*, vol. 41, no. 1, pp. 1–16, 2000.

[6] M. Pillalamarry, S. Harpalani, and S. Liu, "Gas diffusion behavior of coal and its impact on production from coalbed methane reservoirs," *International Journal of Coal Geology*, vol. 86, no. 4, pp. 342–348, 2011.

[7] G. Chen, *Gas Slippage and Matrix Shrinkage Effects on Permeability of Coal*, The University of Arizona, 1994.

[8] W. K. Sawyer, G. W. Paul, and R. A. Schraufnagel, *Development and application of a 3-D coalbed simulator*, Annual Technical Meeting, June 10 - 13, Calgary, Alberta, Petroleum Society of Canada, 1990.

[9] J. R. Seidle and L. G. Huitt, "Experimental measurement of coal matrix shrinkage due to gas desorption and implications for cleat permeability increases," in *Proceeding of International Meeting on Petroleum Engineering*, pp. 575–582, Beijing, November 1995.

[10] P. Q. Huy, K. Sasaki, Y. Sugai, and S. Ichikawa, "Carbon dioxide gas permeability of coal core samples and estimation of fracture aperture width," *International Journal of Coal Geology*, vol. 83, no. 1, pp. 1–10, 2010.

[11] Y. Liang, "Coal mine methane drainage technology in Huainan coal mining area," *China Coalbed Methane*, vol. 3, no. 1, pp. 7–9, 2006.

[12] Z. S. Shi, B. Liang, Y. Wang, and B. Qin, "Deformation characteristics of gas drainage borehole in loading and unloading," *Journal of the China Coal Society*, vol. 42, pp. 1458–1465, 2017.

[13] G. Z. Yin, B. He, M. H. Li, J. Cao, H. Qin, and W. P. Li, "Coupling mechanism between flow rate of gas drainage and coal seam abutment stress under mining conditions," *Meitan Xuebao/journal of the China Coal Society*, vol. 40, pp. 736–741, 2015.

[14] Y. G. Wang, H. Y. Li, Q. X. Qi, Y. W. Peng, C. R. Li, and Z. G. Deng, "The evolution of permeability and gas extraction technology in mining coal seam," *Journal of China Coal Society*, vol. 35, pp. 406–410, 2010.

[15] D. J. Xue, H. W. Zhou, X. L. Tang, and Y. F. Zhao, "Mechanism of deformation-induced damage and gas permeability enhancement of coal under typical mining layouts," *Chinese Journal of Geotechnical Engineering*, vol. 35, pp. 328–336, 2013.

[16] Q. Wei, X. U. Jia-Lin, and X. Y. Peng, "Experimental study of coupling between solid and gas during drainage by advance pressure relief in mining-coal seam," *Journal of China University of Mining & Technology*, vol. 41, pp. 900–905, 2012.

[17] M. Y. Weng, J. H. Xu, and C. Li, "Relationship of coal and rock damage, underground behavior and methane gushing in fully mechanized caving mining face," *Journal of China Coal Society*, vol. 36, pp. 1709–1714, 2011.

[18] H. F. Wang, Y. P. Cheng, W. U. Dong-Mei, and H. Y. Liu, "Gas emission and parameter optimization of gas extraction in mining face of short distance protective seam," *Journal of China Coal Society*, vol. 35, pp. 590–594, 2010.

[19] Y. U. Ming-Gao, J. K. Chao, T. X. Chu, F. Teng, and L. I. Pin, "Experimental study on permeability parameter evolution of pressure-bear broken coal," *Journal of China Coal Society*, vol. 42, pp. 916–922, 2017.

[20] X. Su, Y. Feng, J. Chen, and J. Pan, "The characteristics and origins of cleat in coal from Western North China," *International Journal of Coal Geology*, vol. 47, no. 1, pp. 51–62, 2001.

[21] S. W. Webb, "Gas transport mechanisms," in *Gas Transport in Porous Media*, C. K. Ho and S. W. Webb, Eds., vol. 20 of Theory and Applications of Transport in Porous Media, pp. 5–26, Springer, Dordrecht, 2006.

[22] Q. Liu, Y. Cheng, T. Ren, H. Jing, Q. Tu, and J. Dong, "Experimental observations of matrix swelling area propagation on permeability evolution using natural and reconstituted samples," *Journal of Natural Gas Science and Engineering*, vol. 34, pp. 680–688, 2016.

[23] M. S. Masoudian, "Multiphysics of carbon dioxide sequestration in coalbeds: a review with a focus on geomechanical characteristics of coal," *Journal of Rock Mechanics and Geotechnical Engineering*, vol. 8, no. 1, pp. 93–112, 2016.

[24] J. E. Santos, "General theory of three-dimensional consolidation," *Esaim Mathematical Modelling & Numerical Analysis*, vol. 20, pp. 49-50, 1986.

[25] M. S. Masoudian, D. W. Airey, and A. el-Zein, "The role of coal seam properties on coupled processes during CO_2 sequestration: a parametric study," *Greenhouse Gases: Science and Technology*, vol. 6, no. 4, pp. 492–518, 2016.

[26] X. Y. Huang and C. L. Jiang, "Study on borehole pressurized sealing technology for gas drainage borehole in mining seam," *Coal Science and Technology*, vol. 39, pp. 45–48, 2011.

[27] T. Xia, F. Zhou, J. Liu, S. Hu, and Y. Liu, "A fully coupled coal deformation and compositional flow model for the control of the pre-mining coal seam gas extraction," *International Journal of Rock Mechanics and Mining Sciences*, vol. 72, pp. 138–148, 2014.

[28] I. Palmer, "Permeability changes in coal: analytical modeling," *International Journal of Coal Geology*, vol. 77, no. 1-2, pp. 119–126, 2009.

[29] J. Q. Shi and S. Durucan, "Drawdown induced changes in permeability of coalbeds: a new interpretation of the reservoir response to primary recovery," *Transport in Porous Media*, vol. 56, no. 1, pp. 1–16, 2004.

[30] X. Cui and R. M. Bustin, "Volumetric strain associated with methane desorption and its impact on coalbed gas production from deep coal seams," *AAPG Bulletin*, vol. 89, no. 9, pp. 1181–1202, 2005.

[31] Z. Pan and L. D. Connell, "Modelling permeability for coal reservoirs: a review of analytical models and testing data," *International Journal of Coal Geology*, vol. 92, pp. 1–44, 2012.

[32] M. S. Masoudian, D. W. Airey, and A. el-Zein, "Mechanical and flow behaviours and their interactions in coalbed geosequestration of CO_2," *Geomechanics and Geoengineering*, vol. 8, no. 4, pp. 229–243, 2013.

[33] Y. Wu, J. Liu, D. Elsworth, X. Miao, and X. Mao, "Development of anisotropic permeability during coalbed methane production," *Journal of Natural Gas Science and Engineering*, vol. 2, no. 4, pp. 197–210, 2010.

[34] H. Y. Liu, "Fully coupled model and engineering application for deformation and pressure-relief gas flow of remote coal and rock mass due to mining," *Journal of China Coal Society*, vol. 36, pp. 1243-1244, 2011.